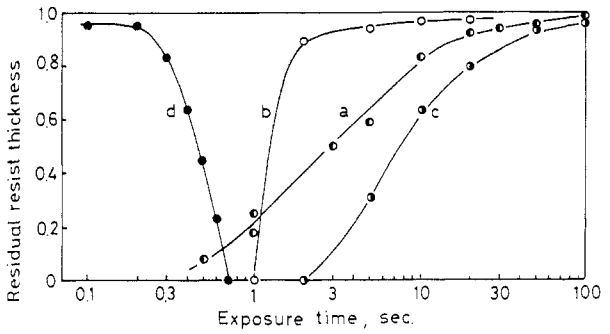

Figure 9. Exposure characteristics of PS-S-12.5: curve a, PS-S-12.5 only; curve b, PS-S-12.5 mixed with CBr_4 (1:1 in weight); curve c, mixture of polystyrene, monomeric spirobenzopyran, and CBr_4 (1:0.5:0.5 in weight); curve d, AZ 1350J.

action back to spiro form of the photogenerated merocyanine during post-exposure baking. The addition of CBr_4 prevents the reverse reaction by generation of a salt or other reaction products with CBr_4.

Monomeric, free spirobenzopyran mixed in polystyrene is also expected to work as a negative resist. Curve c of Figure 9 shows the exposure characteristic curve of the mixture of polystyrene, spirobenzopyran, and CBr_4 (1:0.5:0.5 in weight). The sensitivity and contrast is very poor. This result indicates that incorporation of spirobenzopyran groups to the pendant groups is indispensable to the dissolution rate change by photoirradiation.

Conclusion

The present study has demonstrated that the solubility of polystyrene in cyclohexane can be photocontrolled by incorporating small amounts (~2 mol %) of spirobenzopyran to the pendant groups. The decrease in the solubility is achieved not through interaction among photogenerated merocyanine groups but rather through a decrease of polymer-solvent interaction due to polarity increase of the pendant groups arising from the isomerization of spirobenzopyran. The solubility change resulted in the fractional precipitation. The fractional precipitation was interpreted by the change of molecular weight dependence of critical miscible temperature owing to the configuration of the pendant groups. The copolymer worked as a negative photoresist with high contrast in the presence of CBr_4.

References and Notes

(1) Part 6, Irie, M.; Menju, A.; Hayashi, K. *Nippon Kagaku Kaishi* **1984**, 227.
(2) Irie, M.; Tanaka, H. *Macromolecules* **1983**, *16*, 210.
(3) Irie, M.; Schnabel, W. *Macromolecules* **1985**, *18*, 394.
(4) Irie, M.; Menju, A.; Hayashi, K. *Macromolecules* **1979**, *12*, 1176.
(5) (a) Goldburt, E.; Shvartsman, F.; Fishman, S.; Krongauz, V. *Macromolecules* **1984**, *17*, 1225. (b) Goldburt, E.; Shvartsman, F.; Krongauz, V. *Ibid.* **1984**, *17*, 1876. (c) Krongauz, V. A.; Goldburt, E. S. *Ibid.* **1981**, *14*, 1382.
(6) Kalinsky, Y.; Williams, D. J. *Macromolecules* **1984**, *17*, 292.
(7) Taniguchi, Y.; Hatano, Y.; Shiraishi, H.; Horigome, S.; Nonogaki, S.; Naraoka, K. *Jpn. J. Appl. Phys.* **1979**, *18*, 1143.
(8) Krongauz, V. A.; Goldburt, E. S. *Nature (London)* **1978**, *271*, 43.
(9) (a) McRae, E. G.; Kasha, M. *J. Chem. Phys.* **1958**, *28*, 721. (b) McRae, E. G.; Kasha, M. "Physical Processes in Radiation Biology"; Academic Press: New York, 1964; p 23.
(10) Fox, T. G.; Flory, P. J. *J. Am. Chem. Soc.* **1951**, *73*, 1909, 1915.
(11) Hofer, D. C.; Kaufman, F. B.; Kramer, S. R.; Aviram, A. *Appl. Phys. Lett.* **1980**, *37*, 314.

Quasi-Elastic Light Scattering and Fluorescence Photobleaching Recovery Studies on Poly(lysine) Dynamics

Donald J. Ramsay and Kenneth S. Schmitz*

Department of Chemistry, University of Missouri—Kansas City, Kansas City, Missouri 64110. *Received January 31, 1985*

ABSTRACT: Quasi-elastic light scattering (QELS) and fluorescence photobleaching recovery (FPR) methods were used to study the apparent diffusion coefficient (D_{app}) and the tracer diffusion coefficient (D_{Tr}), respectively, of poly(lysine) of 800 000-dalton molecular weight as a function of [KCl]. The correlation functions from the QELS studies were analyzed by asymptotic analysis and the histogram method with exponential sampling. These analyses indicate that D_{app} splits into two relaxation domains at [KCl] ~ 0.01 M, where the relative values of D_{app} for the two branches differ by over an order of magnitude. In contrast, the added salt profile of D_{Tr} monotonically decreases in value by only a factor of 2 in going from 0.5 M KCl to zero added salt. These observations are discussed in terms of conformational transitions in poly(lysine) and also polyion-small ion and polyion-polyion interactions.

Introduction

Quasi-elastic light scattering (QELS) is a technique that monitors the spontaneous decay of fluctuations in the index of refraction of the medium. It is generally assumed that these fluctuations are due to the decay of concentration gradients of the macromolecules; hence QELS provides a direct measure of the mutual diffusion coefficient (D_m). In the simplest case of center-of-mass translational diffusion in dilute solutions, D_m is proportional to the product of the tracer diffusion coefficient ($D_{Tr} = kT/f$, where kT is the thermal energy and f is the molecular friction factor) and the osmotic compressibility of the solution. Values of D_{Tr} can be obtained from fluorescence photobleaching recovery (FPR) techniques, in which the recovery in fluorescent signal of a bleached region in the solution is monitored. In recent years much attention has been given to solution conditions that induce multiple relaxation modes in the QELS data; hence it is common practice to refer to apparent diffusion coefficients (D_{app}) in the characterization of these decay rates.

The focus of the present study is the diffusion modes of high molecular weight poly(lysine) as inferred from QELS and FPR data. Lin, Lee, and Schurr[1] first reported somewhat bizarre salt concentration (C_s) dependence of D_{app} for this system. After first experiencing an initial rise in value as the concentration of NaBr was decreased to 0.001 M, D_{app} precipitously dropped by over an order of magnitude in value within a narrow range in added salt

0024-9297/85/2218-2422$01.50/0 © 1985 American Chemical Society

concentration. This transition was referred to as an *ordinary–extraordinary phase transition* since the initial increase in D_{app} was consistent with current theories on polyelectrolyte diffusion (ordinary phase) whereas there was no explanation for the rather abrupt change in ionic strength dependence of D_{app} below 0.001 M NaBr (extraordinary phase). Concomitant with the discontinuity in D_{app} these authors also reported a drastic reduction in the total intensity of the scattered light (I_{tils}). The changes in D_{app} and I_{tils} are sufficiently sharp such that a "critical salt concentration" C_c can be defined.

Other physical studies on the poly(lysine) system are not as markedly affected by the added salt concentration. Wilcoxon and Schurr[2] and Ware and co-workers[3,4] used electrophoretic light scattering (ELS) methods to examine the *ordinary–extraordinary phase transition*. The computed values for the electrophoretic mobility (μ) varied from a value of $\mu \sim 3.4 \times 10^{-4}$ cm^2/(V s) to a value of $\mu \sim 6.5 \times 10^{-4}$ cm^2/(V s) from 0.100 M to zero added salt. The data of Wilcoxon and Schurr[2] did, however, suggest a change in $\partial\mu/\partial C_s$ near C_c. Their Figure 11 even suggested a maximum in the value of μ near the value of C_c, although they did not attribute this maximum to any transition phenomenon but rather discussed this observation in terms of *fluctuation* mobilities as observed by classical techniques. These authors further point out that there is no real experimental consensus as to the existence of such a maximum. Ware and co-workers also performed FPR experiments to obtain directly values of D_{Tr}. In contrast to the ionic strength behavior of D_{app}, D_{Tr} exhibited only a mild (~50%), monotonic, decrease in value as the ionc strength was decreased to zero added salt. There emerged, then, an apparent paradox inasmuch as the collective motion of poly(lysine) was drastically reduced through the ordinary–extraordinary phase transition (D_{app} from the QELS results) while the individual poly(lysine) molecules appeared to be totally oblivious to changes in their ionic environment as the added salt concentration was decreased to zero (D_{Tr} from the FPR data). Low shear viscosity data of Martin et al.[5] revealed a small, but significant and reproducible, blip in the vicinity of C_c for the relative viscosity ($\eta_{rel} = \eta_{soln}/\eta_{solv}$) profile. The added salt profile of the apparent conductivity[6] also exhibited a slight change in slope at C_c. It is not clear, therefore, if the behavior of D_{app} at C_c represents a transition from one phase to another; hence we prefer at this time to refer to this phenomenon as a transition from the ordinary *regime* to an extraordinary *regime*, with the abbreviation o–e.

One possible explanation for the o–e behavior of the QELS data is that an expansion in the polyelectrolyte dimensions reduces the effective free volume of the solution; hence the solution dynamics change from that of dilute to semidilute conditions. Comparison of recent studies by Drifford and Dalbiez,[7] on the poly(lysine) and poly(styrenesulfonate) systems, and by Nemoto and coworkers,[8] on the poly(lysine) system, suggest that the above QELS observations do not reflect a dilute–semidilute solution transition. In the case of monovalent salt, Drifford and Dalbiez[7] obtained the following empirical relationship:

$$[C_p^{o-e}b]/[2C_cQ] = 1 \quad (1)$$

where C_p^{o-e} is the concentration of monomeric units of the polyion at the o–e transition point, b is the average distance between charged groups on the polyion, and Q is the Bjerrum length ($Q = e^2/\epsilon kT$, where e is the electron charge and ϵ is the solvent dielectric constant). Nemoto et al.[8] observed that the relaxation processes for poly(lysine) "split" into two relaxation domains and that the condition for the splitting process depended upon both the added salt concentration and the monomeric units of the poly(lysine). These authors reported the following empirical relationship between the poly(lysine) concentration (C_p*) and added salt concentration (C_s*) for splitting to occur:

$$C_p^* = (\text{constant}) \times C_s^{*-0.53} \quad (2)$$

According to eq 1, C_p^{o-e} must increase if one were to increase the value of C_c whereas eq 2 indicates C_p* must decrease in order to increase the value of C_s*. These two studies are apparently observing two different phenomena. The suggestion that Nemoto et al.[8] are observing a process different from those reported previously on poly(lysine) systems is further supported by their observation that the total intensity increases at C_s*, whereas Lin et al.[1] reported a decrease in the total intensity at C_c. Since eq 2 was obtained from data that extended to relatively high polyion concentrations (up to 20 mg/mL), we suggest that the data of Nemoto et al.[8] pertain to a transition from the dilute to the semidilute regimes, and not an observation of the bizarre o–e transition.

We present herein QELS and FPR data on very high molecular weight preparations of poly(lysine) (M_η = 800 000). As in our previous report,[8] two relaxation domains are observed in the QELS data in the transition region. The FPR data confirm the results of Ware and co-workers[3,4] that D_{Tr} is apparently insensitive to this transition.

Materials and Methods

Poly(lysine) was purchased from Sigma Chemical Co. (St. Louis, MO) and used without further purification. The molecular weight of this preparation was 800 000 daltons, as determined by the supplier from viscosity measurements. The degree of polymerization was reported as 3800. The sample was dissolved in doubly distilled water and exhaustively dialyzed against doubly distilled water with the pH adjusted to 7.4. Aliquots of this sample were then dialyzed against the appropriate KCl solutions, pH 7.4. The concentrations of these preparations were determined from optical absorbance using the value A_{240} = 0.1 for a 1 mg/mL solution as determined in our laboratory.[9] For all ionic strengths used in these studies, the poly(lysine) concentration was in the range 2.4–2.8 mg/mL, with the exception of the 0.5 M KCl solution, where the concentration was 3.9 mg/mL.

The QELS facility has been previously described.[9,10] The autocorrelation functions were obtained with a Langley-Ford Model 1096 correlator. The 64-delay point autocorrelation functions were relayed to a Hewlett-Packard 86A microprocessor for storage and analysis. Correlation functions were obtained at several data collection intervals for each of the angles examined.

The FPR experiments were performed in Professor Elliot Elson's laboratory in the Department of Biological Chemistry, Washington University Medical School, St. Louis, MO. The FPR facility has been previously described.[11,12] Poly(lysine) in 0.1 M KCl (pH 8.0) was labeled with fluorescein (1/100 = fluorescein/lysine residue) overnight at room temperature. Aliquots of this solution were then dialyzed against the appropriate KCl solution at pH 7.4. The samples were placed on a microscope slide, the cover glass was sealed, and the slide was mounted in the apparatus. The temperature was maintained at 20 °C and data were collected at several time windows, where the longest elapsed time for any one record of 1000 points was 4 s. Neutral-density filters were used to adjust the intensity of the fluorescence signal. It was also found necessary to use a phosphorescence filter at the shorter time intervals for data collection. In general, 16 records were averaged before numerical characterization.

Data Analysis

QELS. Due to the intrinsic polydispersity in molecular weight of the samples, it is to be expected that the autocorrelation functions are composed of more than one decay function, viz.

$$C(t) = [\sum a_i \exp(-D_i K^2 t)]^2 + B \quad (3)$$

where a_i is the amplitude of the ith component having an effective diffusion coefficient D_i, K is the usual scattering vector, and B is the base line.

Asymptotic Analysis Method. In the asymptotic analysis method,[13,14] data are taken at different collection intervals (Δt) and analyzed as a single-exponential function to obtain an apparent diffusion coefficient valid for a particular number of delay points N; i.e., $D_{app}(N\Delta t)$. A plot of $D_{app}(N\Delta t)$ vs. $N\Delta t$ has as the asymptotic limit at $N\Delta t = 0$ the amplitude-average diffusion coefficient

$$D_{app}(N\Delta t = 0) = \sum a_i D_i \quad (4)$$

where $\sum a_i = 1$. The asymptotic analysis profiles are characterized by a computer fit to the functional form

$$D_{app}(N\Delta t) = D_1 + D_2 \exp(-bN\Delta t) \quad (5)$$

where b is a constant. We therefore have the identities

$$D_{app}(N\Delta t = 0) = D_1 + D_2 \quad (6)$$

and

$$D_{app}(N\Delta t = \infty) = D_1 \quad (7)$$

Histogram Model with Exponential Sampling. The electric field correlation function $g^{(1)}(t)$ is defined in terms of the intensity correlation function $C(t)$ by the equation

$$C(t) = [g^{(1)}(t)]^2 + 1 \quad (8)$$

where

$$g^{(1)}(t) = \int_0^\infty \exp(-\gamma t) G(\gamma)\, d\gamma \quad (9)$$

where $G(\gamma)$ is the distribution function describing the relative amplitudes of the decay modes in γ-space. McWhirter[15] and Pike[16] have shown that the maximum amount of information regarding the form of $G(\gamma)$ is obtained by using exponentially spaced values of γ in the inversion of eq 9. We have used the modification of Fletcher and Ramsay[17] in the analysis of the poly(lysine) data in the present study. In this modification a histogram model is assumed, where a single value of the amplitude acts to represent a region in γ-space. The variables in this method are the number of steps in the histogram, the width of each step, and the center value of γ-space to be examined. After the mean of the distribution is first determined, greater resolution is achieved primarily by reducing the size of each step in γ-space until undesirable features appear, such as negative values, which are indicative of oscillations. Once a suitable histogram is obtained, the number of steps and step size are maintained and additional histograms are generated by shifting the central value of γ. These histograms are then overlayed and averaged to obtain the final histogram representation for the intensity distribution as a function of γ. The intensity distribution as a function of the radius is generated from $G(\gamma)$ through the relationship $G(\gamma)\, d\gamma = L(R)\, dR$, where the histogram representation is maintained by conservation of the area within each step.

FPR. The FPR curves were fit by a least-squares procedure to the functional form

$$F(t) = A - B/(1 + t/\tau_d) \quad (10)$$

where the adjustable parameters A and B are constants related to the magnitude of the unbleached fluorescence signal and the extent of bleaching, respectively, and τ_d is related to the tracer diffusion coefficient by the expression

$$\tau_d = \omega^2/4D_{Tr} \quad (11)$$

where ω is the beam waist of the laser beam.

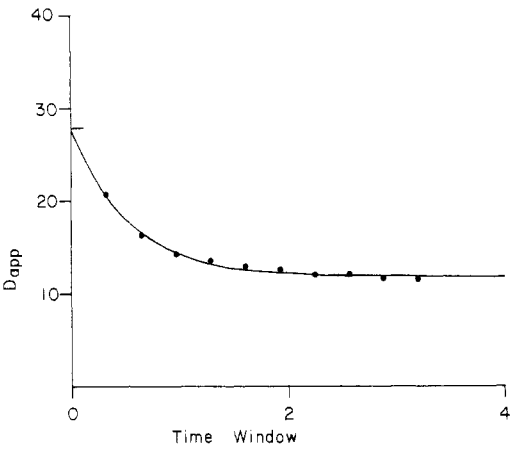

Figure 1. Asymptotic analysis of poly(lysine) in 0.500 M KCl. Values of D_{app} were obtained from a single-exponential analysis of the correlation functions at various data collection intervals (Δt). Plots of D_{app} (in picoficks) vs. time window ($N\Delta t$; in milliseconds) were characterized as an exponential function in accordance with eq 3. The solid curve was generated by the parameters $D_1 = 11.8$ pfick, $D_2 = 16.0$ pfick, and $b = 0.0019$ ms^{-1}.

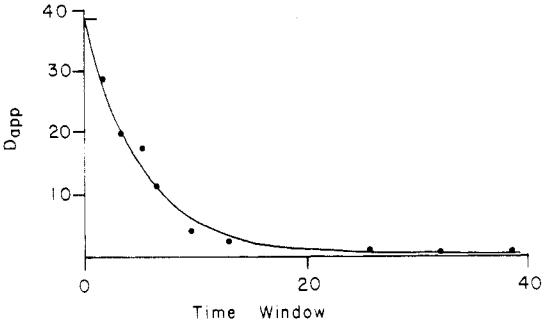

Figure 2. Asymptotic analysis of poly(lysine) in 0.010 M KCl. The solid curve was generated with eq 3 using the parameters $D_1 = 0.35$, $D_2 = 38.0$, and $b = 0.000197$. The units are the same as in Figure 1.

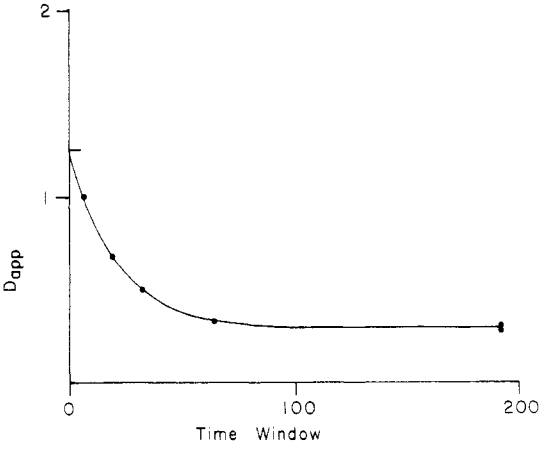

Figure 3. Asymptotic analysis of poly(lysine) in 0.0005 M KCl. The solid curve was generated with eq 3 using the parameters $D_1 = 0.255$, $D_2 = 0.84$, and $b = 0.0000048$. The units are the same as in Figure 1.

Results

Asymptotic analysis plots are presented in Figures 1–3 for the added KCl concentrations of 0.500, 0.01, and 0.0005 M, respectively. Characterization of these data by the functional form of eq 5 is indicated by the solid line. There is no direct theoretical basis for the choice of this functional form other than the fact that it provides the correct power series dependence in the product $N\Delta t$ at the initial

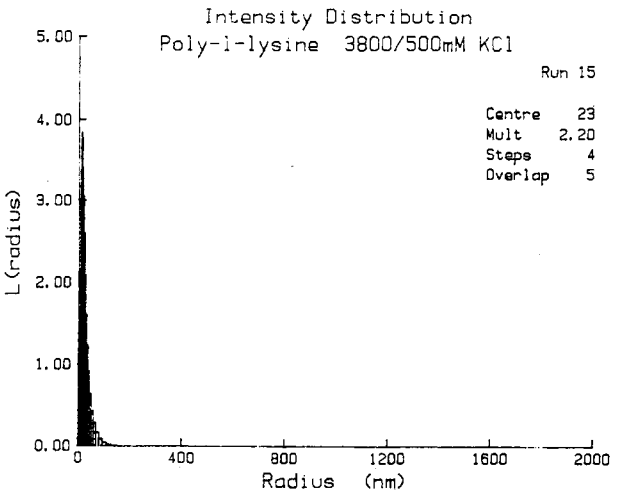

Figure 4. Histogram analysis of poly(lysine) in 0.500 M KCl. Selected correlation functions were analyzed by the histogram method to invert eq 7. The central position, multiplier, number of steps in each histogram, and the number of histograms that were overlapped are given in the figure. The intensity as a function of radius, shown above, was obtained by conservation of the area under the curve; viz., $G(\gamma)\,d\gamma = L(R)\,dR$. These data are those in Figures 5 and 6 were plotted on the same scale to emphasize the range of radii employed in these calculations.

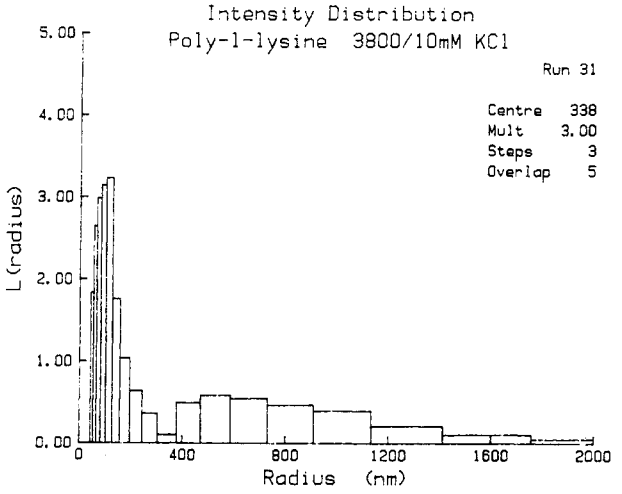

Figure 5. Histogram analysis of poly(lysine) in 0.010 M KCl. The method of analysis and identification of the parameters are described in Figure 4.

rate of decay. There is no provision, therefore, for the possibility of a plateau region at very short elapsed times; thus the value of D_1 may be considered to be an upper limit to $D_{app}(N\Delta t = 0)$. Nonetheless, the data obtained in the 0.010 M KCl solvent clearly show a broad distribution in decay rates as compared to those data obtained in 0.500 or 0.0005 M KCl solvents.

Representative histograms for selected correlation functions obtained for poly(lysine) in 0.500, 0.010, and 0.001 M KCl are presented in Figures 4–6, where the data collection intervals (Δt) are respectively 50, 600, and 500 μs. These time intervals were chosen in these examples because the correlation functions virtually decayed to the base line. The maximum resolution in the distribution obtainable by the histogram method of analysis is strongly dependent on the precision and polydispersity of the experimental points. Therefore, it is significant that the noise on the correlation data was an order of magnitude less in the 0.500 M KCl, 0.100 M KCl, and zero added salt solvents than that at the other salt concentrations. Consequently we were able to recover histogram distributions

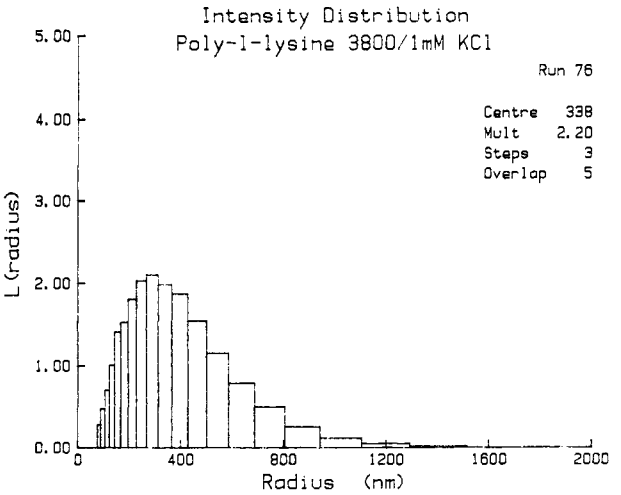

Figure 6. Histogram analysis of poly(lysine) in 0.001 M KCl. The method of analysis and identification of the parameters are described in Figure 4.

Table I
Comparison of Asymptotic and Histogram Methods[a]

D_{app}			
$N\Delta t = 0$	$N\Delta t = \infty$	$\langle\gamma\rangle/K^2$	C_s, M
27.8	11.8	12.2	0.5000
18.2	11.6	15.7	0.1000
38.4	0.4	0.66	0.0100
263.6	0.13	0.61	0.0010
1.1	0.3		0.0005
1.0	0.47	0.45	0.0000

[a] D_{app} was computed from the single-exponential fit of the data and reported as picoficks (10^{-12} m^2/s). Represented in this table are the asymptotic limits of D_{app} for several sets of the QELS data (first two columns), and the average volume $\langle\gamma\rangle$ of the decay rate for a single-relaxation function as analyzed by the histogram method of analysis.

with more steps of narrower width under these conditions. Despite the greater scatter in the data at 0.010 and 0.001 M KCl, we were still able to resolve all but the fine detail present in the intensity distribution. In order to emphasize the range of decay rates, these data were transformed from γ-space to radius space and plotted on the same scale. Except for the 0.010 M KCl concentration data, all of the correlation functions *which could be analyzed by the histogram method* exhibited a unimodal distribution with a mean radius comparable to that computed from D_{app} in the single-exponential analysis. As shown in Figure 5, the histogram analysis of correlation functions in the 0.010 M KCl solvent exhibited a bimodal distribution.

The results of the asymptotic analysis and histogram analysis methods are compared in Table I.

Five representative FPR curves are illustrated in Figure 7, where the elapsed time was 4 s. Data taken at smaller time intervals resulted in smaller values for τ_d, thus suggesting a degree of polydispersity in the sample molecular weight. The values of τ_d and KCl concentrations are given in the figure. These data confirm the earlier studies of Ware and co-workers,[3,4] who reported that the value of D_{Tr} decreased by less than a factor of 2 in going from high values of added salt to essentially salt-free conditions.

Discussion

The data presented herein extend to much higher molecular weight preparations the rather bizarre added salt profile of D_{app} for poly(lysine).[1-4,7] This abrupt decrease in the value of D_{app} cannot be attributed entirely to an expansion in the poly(lysine) dimensions since D_{Tr} de-

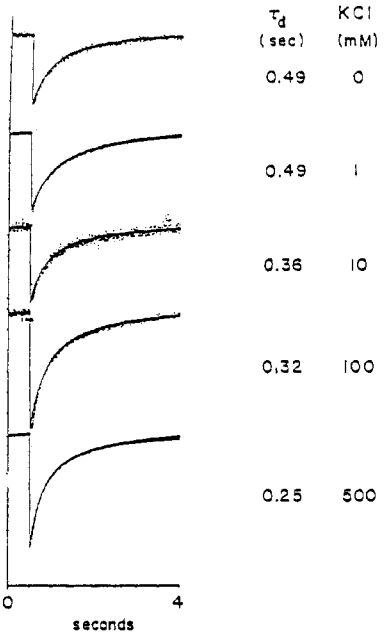

Figure 7. Fluorescein-labeled poly(lysine) was used in the PFR experiments to obtain the tracer diffusion coefficient as a function of added salt concentration. The FPR recovery times computed from eq 10 and the corresponding added KCl concentrations are given at the respective curves.

creases by only ~50% in going from 0.1 to 0.001 M added salt (cf. Figure 7).

FPR. We first direct attention to the increase in the apparent molecular friction factor of poly(lysine) as inferred from the added salt dependence of D_{Tr}. Perhaps the most popular interpretation is that the polyion undergoes a change in geometry as the ionic strength is lowered, which in turn increases the degree of hydrodynamic dissipation in the system. This increase in hydrodynamic friction may occur through either a symmetric expansion of the polyion dimensions (i.e., swelling of the polyion) or a distortion in the symmetry of the polyion at constant molecular volume (i.e., sphere-to-rod transition). An alternative interpretation, which does not require a change in the polyion dimensions, is that electrolyte dissipation becomes increasingly important as the ionic strength is lowered. That is, polarization of the associated ion cloud tends to retard the progress of the polyion through the solution.

In order to examine these three models in detail, we represent the FPR data obtained in our laboratory and those of Zero and Ware[4] in terms of the friction ratio

$$f/f_H = D_{Tr,H}/D_{Tr} = \tau_d/\tau_{d,H} \quad (12)$$

where D_{Tr} (τ_d) is the value of the tracer diffusion coefficient (FPR time) at the added salt concentration and $D_{Tr,H}$ ($\tau_{d,H}$) is the value of D_{Tr} (τ_d) at the highest added salt concentration employed in the respective studies. These ratios are summarized in Table II.

Conformational Change. In the case of a semiflexible polyelectrolyte, the change in the geometry of the polyion is effected through the electrostatic part of the persistence length (P).[18-20] The parameter P is represented as a sum of two terms, the intrinsic persistence length P_0 and the electrostatic component P_{el}

$$P = P_0 + P_{el} \quad (13)$$

This increase in P may either increase the effective hydrodynamic volume by expansion along each axis by an amount proportional to the molecular axis (swelling) or lead to a greater molecular asymmetry at a fixed hydrodynamic volume by expansion along one axis and contraction along another. In the former case the distribution function for the segment remains unaltered but the local density of the segments is reduced. The latter case is supported by Monte Carlo calculations[21] in which an increase in the step length (due to an increase in P) requires a decrease in the number of steps and a decrease in the symmetry of the segment distribution.

Table II
Friction Factor Ratios

C_s, M	D_{Tr}[a]	$D_{Tr,H}$[b]/D_{Tr}	$\tau_d/0.25$[c]
0.000	41.1	1.62	1.88
0.001			1.96
0.002	54.0	1.23	
0.004	59.0	1.13	
0.006	64.0	1.04	
0.010	60.3	1.11	1.44
0.020	63.2	1.05	
0.100			1.28
0.500			1.00

[a] From ref 4, where the values of D_{Tr} are in units of picoficks (10^{-12} m^2/s). [b] We determined the value of $D_{Tr,H}$ from the intercept of D_{Tr} vs. $1/C_s$, where D_{Tr} are the values reported in ref 4. [c] Cf. Figure 7.

We adopt the simplest model of a random flight coil for the symmetric expansion of poly(lysine) upon lowering the added salt concentration. The ratio of hydrodynamic radii at two ionic strengths therefore obeys the relationship

$$(R_1/R_2)^2 = P_1/P_2 \quad (14)$$

where R_i is the equivalent hydrodynamic radius under the added salt condition denoted by the subscript i and it is assumed that the radius of gyration is proportional to the effective hydrodynamic radius. If 1 and 2 correspond to the two added salt extremes, then eq 14 suggests that the persistence length must increase by a factor of ~4 to be in accordance with the data given in Table II.

In the evaluation of P_{el}, one must consider the possibility of counterion condensation on the linear array of charges.[20,22,23] Manning,[20] working with the linearized Poisson–Boltzmann equation, and Russel,[22] working with the nonlinear Poisson–Boltzmann equation, reached the mutual conclusion that small-ion condensation will occur to the extent that the linear charge density becomes equal to, or less than, $1/Q$, where Q is the Bjerrum length. Since the charge groups in poly(lysine) are separated by a distance of ~3.6 Å along the backbone contour, counterion condensation should therefore occur in this system to the extent that the average spacing between effective unit charges is approximated as $Q \sim 7$ Å at 20 °C.

If the interaction between charged groups in a fixed linear array is weak, then the potential of mean force is a good approximation for the pairwise interaction between the n charged groups. P_{el} then takes on the following form:[18,19]

$$P_{el} = Q/4b^2\kappa^2 \sim 1/4Q\kappa^2 \quad (15)$$

where κ is the Debye–Hückel screening parameter and b is the average spacing between adjacent charges along the contour of the polyion, which was set equal to Q to account for counterion condensation. It is noted that eq 15 predicts that P_{el} is proportional to $1/C_s$.

Manning[20] obtained the following expression for the electrostatic part of the persistence length:

$$P_{el} = -a_2 \log (C_s) \quad (16)$$

where a_2 is a parameter to be determined from experiment.

We interpret the FPR data in Table III for 0.001 and 0.1 M KCl in terms of eq 15 and 16. Using eq 15 with the

Table III
Electrolyte Dissipation Charge[a]

[KCl], M	$(f_H + f_{ed})/f_H$	$D^b_{composite}$	Z
0.0100	1.44		255[c]
0.0010	1.96		226[c]
0.5000		13.2	194[d]
0.1000		17.7	194[d]
0.0100		61.7	194[d]
0.0010		253.3	194[d]

[a] The fixed parameters in these calculations are $a_p = 176 \times 10^{-8}$ cm, $D_s = 1 \times 10^{-5}$ cm^2/s, $\eta = 0.01$ P, $\epsilon = 80$, and $T = 293$ and K. [b] Units of picoficks (10^{-12} m^2/s). [c] Computed from eq 20, where the only adjustable parameter Z is constrained to the equivalence $(f_H + f_{ed})/f_H = \tau_d/0.25$, where the ratio of FPR times is given in Table II. [d] Computed from eq 21 and 22, where the only adjustable parameter Z is constrained to provide the best fit for all of the values of $D_{app}(N\Delta t = 0)$ given in Table I for [KCl] > 0.001 M. The optical absorbance in these calculations was $A_{240} = 0.25$ for all salt concentrations except [KCl] = 0.500, where $A_{240} = 0.39$. The values of C_p were estimated from the molar extinction coefficient of 0.1 L/g and the molecular weight of 800 000 daltons.

value $Q = 7$ Å, we calculate $P_{el} = 357$ Å ($1/\kappa = 100$ Å for 0.001 M KCl) and $P_{el} = 3.57$ Å ($1/\kappa = 10$ Å for 0.1 M KCl). Using these values of P_{el} in eq 13 and the experimental ratio R_1/R_2, we compute from eq 14 an intrinsic persistence length $P_0 \sim 260$ Å. We now compute the experimental ratio P_0/a_2 using eq 13 and 16 for these two salt conditions. Our empirical result is $P_0 = 0.49a_2$. It is noted that Manning obtained the relationship $P_0 = (221/559)a_2 = 0.39a_2$ for DNA (cf. eq 83 of ref 20).

We now estimate a value for the intrinsic persistence length P_0 using the QELS data for [KCl] = 0.5 M, where eq 15 and 16 suggest $P_{el} \sim 0$ for [KCl] = 0.5 M. We use the relationship between the hydrodynamic radius a_p and the contour length L as given by Flory[24] on the basis of the Kirkwood–Riseman[25] result for a random-coil polymer

$$\langle L(2P_0)\rangle^{1/2} = ((6^{1/2})\pi/5.11)a_p = 1.5a_p \quad (17)$$

If the average spacing between lysine residues is 3.6 Å and the degree of polymerization is 3800, then the contour length for the poly(lysine) used in the present study is $L = 3800 \times 3.6 = 13\,680$ Å. The histogram value of $\langle\gamma\rangle/K^2 = 1.22 \times 10^{-7}$ cm^2/s (cf. Table I) results in the value $a_p = 176$ Å. The estimated value of P_0 from eq 17 is therefore $P_0 \sim 4$ Å. A similar calculation on the data of Lin et al.[1] for $a_p = 140$ Å and $L = 960 \times 3.6$ Å $= 3456$ Å results in a value $P_0 \sim 9$ Å. The discrepancy between these two values of P_0 computed from QELS data may be due to the different salt and poly(lysine) concentrations employed (Lin et al. were at 1.0 M NaBr and extrapolated their results to infinite dilution). The osmotic compressibility factor would therefore be more important in our studies at finite polyion concentrations and thus result in D_{app} values that are larger than the infinite dilution limit (cf. section entitled "Electrolyte Dissipation"). The two studies are nonetheless in agreement as to the estimated order of magnitude of P_0, which is considerably smaller than P_0 estimated from eq 14 using the FPR data. In view of the small value of P_0 relative to the contour length of poly(lysine), one might suspect the validity of computations based on expressions derived in the rigid-rod limit.

It is significant that the value of P_0 computed from the FPR data over a wide range of added salt concentrations is *much larger* than P_0 computed from QELS data in the high-salt limit. This suggests to us that friction sources other than of hydrodynamic origin are important in the description of poly(lysine) in low ionic strength solvents. Discussion of one possible source, electrolyte dissipation, is deferred to the following section.

The second model involving a conformational change requires that the total volume of the particle remain constant. We assume a change in conformation from a sphere to prolate ellipsoid to maximize the change in friction, where the fixed-volume requirement provides a relationship between the spherical radius a_p and the semimajor axis (A) and semiminor axis (B)

$$(a_p)^3 = A^2B \quad (18)$$

We use the value $a_p = 176$ Å computed from the QELS data on poly(lysine) in 0.5 M KCl. The ratio f/f_H obtained from experiment can then be used to obtain a value for the ratio $X = A/B$[26]

$$f/f_H = [X\{X^2 - 1\}]^{1/2}/[\ln (X + \{X^2 - 1\}^{1/2})] \quad (19)$$

With this procedure, the ratio $f/f_H = 1.88$ results in the values $A/B \sim 18$, $A \sim 460$ Å, and $B \sim 25.5$ Å. Since the assumption that the poly(lysine) has spherical symmetry in the high-salt regime may be in error, these calculations therefore represent *minimum* asymmetric dimensions for the prolate ellipsoid in the extraordinary regime. If the shape of the molecule was also asymmetric in the ordinary regime, then the ratio A/B would have to be much larger than 18 in the extraordinary regime to explain the observed change in D_{Tr}. While the decrease in D_{Tr} can be interpreted in terms of an ionic strength induced conformational change to a more asymmetric shape, the magnitude of the change, as suggested by these calculations, should also produce a change in the optical properties of the system. Martin et al.[5] could not detect significant depolarized scattering through the transition region. Failure to observe significant depolarized scattering does not, unfortunately, rule out the possibility of a symmetric–asymmetric conformational change if the poly(lysine) has an intrinsically low anisotropy.

It is of interest to note that Stigter[27] attempted an analysis of the QELS data of Lin et al.[1] in terms of a coil-to-rod transition, where direct repulsive pairwise interactions between neighboring rods were incorporated in the second virial coefficient as an effective rod diameter. The theory employed was found to predict an ordered phase at a poly(lysine) concentration $\sim 1/3$ that observed experimentally for the ordinary–extraordinary phase transition. It was suggested that rotational restrictions and many-body interactions may account for the difference between theory and experiment. Nonetheless, failure to observe a conformational transition by birefringence[5] and conductivity[6] measurements tend to rule out large changes in the conformation of poly(lysine) through the transition region.

Electrolyte Dissipation. An increase in the apparent molecular friction factor upon a decrease in the added salt does not necessarily have to be associated with a change in the polyion dimensions. The additional source of friction may be due to electrolyte dissipation (small ion–polyion coupled dynamics).[28-30]

In order to obtain a quantitative assessment of the importance of electrolyte dissipation effects, we employ the analytical expression derived by Schurr[29] for an asymmetric distribution of small ions about a semipermeable gel sphere

$$f = 6\pi\eta a_p + [(Ze/a_p)^2/12\epsilon\kappa D_s] \times [1 - (1 + 2a_p\kappa)\exp(-2a_p\kappa)] = f_H + f_{ed} \quad (20)$$

where Z is the effective charge of the polyion, D_s is the diffusion coefficient for the small ions, f_H is the hydrodynamic dissipation component, f_{ed} is the electrolyte dissipation component, and the remaining parameters have been defined previously. The ratio of FPR times given in

Table II for the current study is used to determine the electrolyte dissipation charge Z from the ratio $(f_H + f_{ed})/f_H$. The fixed parameters in this exercise are the polyion radius (176 Å), the small-ion diffusion coefficient ($D_s = 1 \times 10^{-5}$ cm^2/s), the solvent viscosity ($\eta = 0.01$ P), and the dielectric constant ($\epsilon = 80$). The results, along with the analysis of the QELS data to be discussed in the next section, are summarized in Table III. Since the QELS data are also interpreted in terms of small-ion coupling effects, further discussion of electrolyte dissipation effects are deferred until after analysis of the QELS data.

QELS. Lin, Lee, and Schurr[1] proposed a small ion–polyion coupled-mode theory to interpret the ionic strength behavior of D_{app} in the ordinary regime, where D_{app} has the following form:

$$D_{app} = (1/2)[D_p(1 - \Omega) + D_s(1 + \Omega)] \quad (21)$$

where D_p is the polyion diffusion coefficient and

$$\Omega = \frac{D_p - D_s[1 + (2C_s/C_pZ)]/Z}{D_p + D_s[1 + (2C_s/C_pZ)]/Z} \quad (22)$$

Trivant et al.[31] extended this theory to include counterions and co-ions that might differ in their mobilities. Their theory reduces to eq 21 and 22 for the special case when these small-ion mobilities are identical, as in the present study for K^+ and Cl^-. It is also noted that eq 21 and 22 reduce to the expression of Berne and Pecora[32] for $C_pZ \ll C_s$ and to the expression of Stephen[33] in the dual limits $D_pZ \ll D_s$ and $C_pZ \ll C_s$. The value of D_p is identified with D_{Tr}; hence internal consistency with the analysis of the FPR data in terms of electrolyte dissipation effects suggests the theoretical expression

$$D_p = kT/(f_H + f_{ed}) \quad (23)$$

where $f_H + f_{ed}$ is defined by eq 20. Since the resulting expression for D_{app} as given by eq 20–23 is a synthesis of two theories, we refer to the resulting expression as a composite diffusion coefficient denoted by $D_{composite}$. As in the case with the FPR analysis, all of the molecular parameters are fixed except the apparent charge Z. Assuming that the theoretical expression of $D_{composite}$ as defined by eq 20–23 is to be identified with the experimental asymptotic limit $D_{app}(N\Delta t = 0)$, we have attempted to fit the data in Table I with eq 20–23 with the single adjustable parameter Z. The results of these calculations are given in Table III.

We believe it is encouraging that the added salt behavior of both the FPR and QELS data is adequately characterized by a single set of molecular parameters: $190 < Z < 240$ with the constraint $a_p = 176$ Å. Since both Z and a_p may vary over the ionic strength range examined, the relatively narrow range of values for Z at fixed a_p suggests that any dependence of a_p on ionic strength must be weak. This conclusion is also supported by recent Monte Carlo calculations of Zimm and Le Bret[23,34] on the distributions of small ions about cylinders and planes. These authors suggest that, for these specific geometries, there exists a certain number of counterions within a distance R from the charged surface which cannot be diluted away from the surface even when the bulk concentration reduces to zero. The interaction between segments of the cylindrically shaped polyion is therefore not exposed to the bulk solvent ionic strength as the surface charges are buffered by the sheath of counterions. Furthermore, for a cylinder of intracharge spacing $b = 1.7$ Å as in DNA, the "local" concentration of counterions can reach as high as 2 M.[34] It is for this reason, therefore, that the substitution of $b = Q$ remains valid as an ad hoc correction approximation. It necessarily follows that the dynamics of the charged cylinder as it moves through a polar solvent must include the dynamics of the surrounding ion cloud, the composition of which appears to be independent of the ionic strength of the medium. Calculations of the persistence length of polyelectrolytes based on hydrodynamic data should therefore be suspect if this, or other, source of nonhydrodynamic dissipation is not taken into consideration. It is not valid, therefore, to conclude a polyion expands simply because hydrodynamic methods indicate that the apparent friction factor increases. If the polyion does expand as the ionic strength is lowered, then, within the context of the electrolyte dissipation theory of Schurr, the value of the parameters Z will also increase since they appear as a ratio (viz., ZD_p).

In view of the reported degree of polymerization (3800), the effective charge Z seems to be anomalously small. This reduction in apparent charge may be a physical effect due to the associated ion cloud, where the diffusing entity of the polyion–small ion is in osmotic equilibrium with the bulk solution. The small value of Z may also suggest inadequacies in the current stage of theoretical development in the description of polyion dynamics. For example, Geigenmuller[35] compared the electrolyte dissipation charge obtained from Schurr's theory[29] with the apparent charge obtained from Booth's theory[30] in his reanalysis of the Lin, Lee, and Schurr data.[1] Geigenmuller observed that Booth's theory gave a charge 2–3 times larger than Schurr's theory. He concluded that hydrodynamic interaction, present in Booth's theory but not in Schurr's approximation, had to be compensated for with a larger polyion charge in order to attain the same decrease in the apparent friction factor. Schurr[36] responded that the two theories represented opposite extremes since Booth did not consider dissipation effects of nonhydrodynamic origin. Schurr therefore suggested that Booth's theory overestimated the apparent charge whereas Schurr's theory probably underestimated the apparent charge. The apparent charge Z is therefore a parameter which may "mask" other phenomena. If this is the case, then the additional processes to be included in these theories would act in a direction opposite to those already considered. The coupled-mode theories of Lin, Lee, and Schurr[1] and of Tivant et al.,[31] and those to which they reduce,[32,33] suffer from the same omissions.

We have previously proposed that the "extraordinary regime" suggested by light scattering methods may be due to nonlinear small-ion effects on both the scattering power and the dynamics of the polyions.[9] Briefly, the anomalously slow relaxation process is proposed to result when the ion clouds of neighboring polyions begin to overlap. The more loosely associated small ions are then "shared" by two or more polyions and attempt to diffuse under the cummulative influence of the electric fields of the polyions. The result is a fluctuating dipole field that tends to retard the relative motions of the participating polyions. That is, the polyions within the "temporal aggregate" are no longer to be considered as independent (or even weakly coupled) statistical units. The interpretation of the QELS data in the "ordinary regime" and the FPR data throughout the entire ionic strength range examined as being primarily due to small-ion effects provides, in our opinion, a self-consistent picture of poly(lysine) dynamics throughout the entire ionic strength range.

One final comment regarding the definition of a "fick" as a unit of diffusivity. To our knowledge, Gordon et al.[37] first introduced this unit as being 10^{-7} cm^2/s. This definition as they proposed is in the spirit of the Svedberg unit

(10^{-13} s) and is a convenient unit for diffusitivities of biopolymers in aqueous solvents and in computing the molecular weight from the Svedberg equation. Diffusivities, however, span a much wider range of values, over several orders of magnitude in going from the gas to the glassy state, than do sedimentation coefficients. Furthermore, as pointed out by Professor Stockmayer, the 10^{-7} cm^2/s unit is not consistent with the SI system (personal communication). Upon his suggestion we have therefore defined the fick as 1 m^2/s.

Conclusions

On the basis of the information presented in this paper, it is concluded that small ion–polyion coupled dynamics are largely responsible for the QELS and FPR observations of poly(lysine) over the added salt range 0.5–0.001 M. In view of the anomalously small value of the effective polyion charge Z (compared to the degree of polymerization), it is concluded that either this parameter has physical significance in describing a small ion–polyion unit in osmotic equilibrium with the bulk solution or both the coupled-mode theory and the electrolyte dissipation theory suffer from the same inadequacies in describing the dynamic processes in solution.

Acknowledgment. We extend our gratitude to Professor Elliot Elson for providing time on his FPR facility and the subsequent characterization of the data. We also acknowledge stimulating discussions with Professor Schurr on the electrostatic contribution to the persistence length of flexible polyelectrolytes and correspondence with Professor Stockmayer on the notation of diffusivity. This research was supported by a grant from the National Science Foundation (Grant PCM-8118378).

Registry No. KCl, 7447-40-7; poly(lysine) (homopolymer), 25104-18-1; poly(lysine) (SRU), 38000-06-5.

References and Notes

(1) Lin, S.-C.; Lee, W. I.; Schurr, J. M. *Biopolymers* **1978**, *17*, 1041.
(2) Wilcoxon, J. P.; Schurr, J. M. *J. Chem. Phys.* **1983**, *78*, 3354.
(3) Ware, B. R.; Cyr, D.; Gorti, S.; Lanni, F. In "Measurement of Suspended Particles by Quasi-Electric Light Scattering"; Dahneke, B. E., Ed.; Wiley-Interscience: New York, 1983; Chapter 9, p 255.
(4) Zero, K.; Ware, B. R. *J. Chem. Phys.* **1984**, *66*, 1610.
(5) Martin, N. B.; Tripp, J. B.; Shibata, J. H.; Schurr, J. M. *Biopolymers* **1979**, *18*, 2127.
(6) Shibata, J.; Schurr, J. M. *Biopolymers* **1979**, *78*, 3354.
(7) Drifford, M.; Dalbiez, J.-P. *Biopolymers*, in press.
(8) Nemoto, N.; Matsuda, H.; Tsunashima, Y.; Kurata, M. *Macromolecules* **1984**, *17*, 1731.
(9) Schmitz, K. S.; Lu, M.; Singh, N.; Ramsay, D. J. *Biopolymers* **1984**, *23*, 1637.
(10) Schmitz, K. S.; Lu, M.; Gauntt, J. *J. Chem. Phys.* **1983**, *78*, 5059.
(11) Koppel, D. E.; Axelrod, D.; Schlessinger, J.; Elson, E. L.; Webb, W. *Biophys. J.* **1976**, *16*, 1315.
(12) Icenogle, R. D.; Elson, E. L. *Biopolymers* **1983**, *22*, 1949.
(13) Schmitz, K. S.; Pecora, R. *Biopolymers* **1975**, *14*, 521.
(14) Schmitz, K. S.; Parthasarathy, N.; Kent, J. C.; Gauntt, J. *Biopolymers* **1982**, *21*, 1365.
(15) McWhirter, J. G. *Opt. Acta* **1980**, *27*, 83.
(16) Pike, E. R. In "Scattering Techniques Applied to Supramolecular and Nonequilibrium Systems"; Chen, S.-H., Chu, B., Nossal, R., Eds.; Plenum Press: New York, 1981; p 179.
(17) Fletcher, G. C.; Ramsay, D. J. *Opt. Acta* **1983**, *30*, 1183.
(18) Skolnick, J.; Fixman, M. *Macromolecules* **1977**, *10*, 944.
(19) Odjik, T. *J. Polym. Sci., Polym. Phys. Ed.* **1977**, *15*, 477.
(20) Manning, G. J. *Q. Rev. Biophys.* **1978**, *11*, 179.
(21) Šolc, K.; Stockmayer, W. H. *J. Chem. Phys.* **1971**, *54*, 2756.
(22) Russel, W. B. *J. Polym. Sci., Polym. Phys. Ed.* **1982**, *20*, 1233.
(23) Le Bret, M.; Zimm, B. H. *Biopolymers* **1984**, *23*, 271.
(24) Flory, P. J. "Principles of Polymer Chemistry"; Cornell University Press: Ithaca, NY, 1967; Chapter XIV.
(25) Kirkwood, J. G.; Riseman, J. *J. Chem. Phys.* **1948**, *16*, 565.
(26) Van Holde, K. E. "Physical Biochemistry", 2nd ed.; Prentice-Hall: Englewood Cliffs, NJ 1985; p 95.
(27) Stigter, D. *Biopolymers* **1979**, *18*, 3125.
(28) Booth, F. *J. Chem. Phys.* **1954**, *22*, 1956.
(29) Schurr, J. M. *Chem. Phys.* **1980**, *45*, 119.
(30) Imai, N.; Mandel, M. *Macromolecules* **1982**, *15*, 1562.
(31) Trivant, P.; Turq, M.; Drifford, M.; Magdelenat, H.; Menez, R. *Biopolymers* **1983**, *22*, 643.
(32) Berne, B. J.; Pecora, R. "Dynamic Light Scattering"; Wiley: New York, 1976; p 212.
(33) Stephen, M. J. *J. Chem. Phys.* **1971**, *55*, 3878.
(34) Zimm, B. H.; Le Bret, M. *J. Biomol. Struct. Dynamics* **1983**, *1*, 461.
(35) Geigenmuller, U. *Chem. Phys. Lett.* **1984**, *110*, 666.
(36) Schurr, J. M. *Chem. Phys. Lett.* **1984**, *110*, 668.
(37) Gordon, V. A.; Knobler, C. M.; Olins, D. E.; Schumaker, V. N. *Proc. Natl. Acad. Sci. U.S.A.* **1978**, *75*, 660.